Contact
Volume 4: 1–13

DOI: 10.1177/2515256421042456
journals.sagepub.com/home/ctc
SAGE

Impact of Intrinsic and Extrinsic Factors on Cellular Sphingomyelin Imaging with Specific Reporter Proteins

Toshihide Kobayashi [1,2,3], Nario Tomishige[1,2,3], Takehiko Inaba[1], Asami Makino[1], Michio Murata[4,5], Akiko Yamaji-Hasegawa[1] and Motohide Murate[1,2,3]

Abstract

Sphingomyelin (SM) is a major sphingolipid in mammalian cells. Although SM is enriched in the outer leaflet of the cell plasma membrane, lipids are also observed in the inner leaflet of the plasma membrane and intracellular organelles such as endolysosomes, the Golgi apparatus and nuclei. SM is postulated to form clusters with glycosphingolipids (GSLs), cholesterol (Chol), and other SM molecules through hydrophobic interactions and hydrogen bonding. Thus, different clusters composed of SM, SM/Chol, SM/GSL and SM/GSL/Chol with different stoichiometries may exist in biomembranes. In addition, SM monomers may be located in the glycerophospholipid-rich areas of membranes. Recently developed SM-binding proteins (SBPs) distinguish these different SM assemblies. Here, we summarize the effects of intrinsic factors regulating the lipid-binding specificity of SBPs and extrinsic factors, such as the lipid phase and lipid density, on SM recognition by SBPs. The combination of different SBPs revealed the heterogeneity of SM domains in biomembranes.

Keywords

lipid imaging, lipid-binding protein, pore-forming toxin, lipid domain, cholesterol, lipid raft

Introduction

Sphingomyelin (SM) (Figure 1A) is a major sphingolipid in mammalian cells. SM is distributed ubiquitously in the animal body and SM is enriched in the outer leaflet of the cell plasma membrane. However, SM is also observed in the inner leaflet of the plasma membrane (Murate et al., 2015) and intracellular organelles such as endolysosomes (Makino et al., 2015, 2017), the Golgi apparatus (Bakrac et al., 2010; Deng et al., 2016) and nuclei (Lazzarini et al., 2015). In the outer leaflet of the plasma membrane, SM forms specific lipid raft domains together with cholesterol (Chol; Levental et al., 2020; Lingwood & Simons, 2010). Lipid rafts are postulated to be involved in a number of pathophysiological events. Compared to the role of SM in cell surface lipid domains, little is known about the role of intracellular SM. However, recent results suggest that intracellular SM has important pathophysiological roles (Ellison et al., 2020).

Measuring the localization of endogenous SM is essential to understand the physiological role of the lipid. The proposed size of lipid rafts is in the range of the submicron scale. However, methods to visualize SM at the submicron scale in a leaflet-specific manner are limited. The recent discoveries of SM-binding proteins (SBPs) enabled visualization of endogenous SM at the submicron scale (Kishimoto et al., 2016; Tomishige et al., 2021; Yamaji-Hasegawa et al., 2016).

[1]Lipid Biology Laboratory, RIKEN, Wako, Saitama, Japan
[2]Cellular Informatics Laboratory, RIKEN CPR, Wako, Saitama, Japan
[3]Laboratoire de Bioimagerie et Pathologies, Faculté de Pharmacie, UMR 7021 CNRS, Université de Strasbourg, Illkirch, France
[4]Department of Chemistry, Graduate School of Science, Osaka University, Toyonaka, Osaka, Japan
[5]ERATO, Lipid Active Structure Project, Japan Science and Technology Agency, Graduate School of Science, Osaka University, Osaka, Japan

Corresponding Author:
Toshihide Kobayashi, Laboratoire de Bioimagerie et Pathologies, UMR 7021 CNRS, Université de Strasbourg, Faculté de Pharmacie, 67401 Illkirch, France.
Email: toshihide.kobayashi@unistra.fr

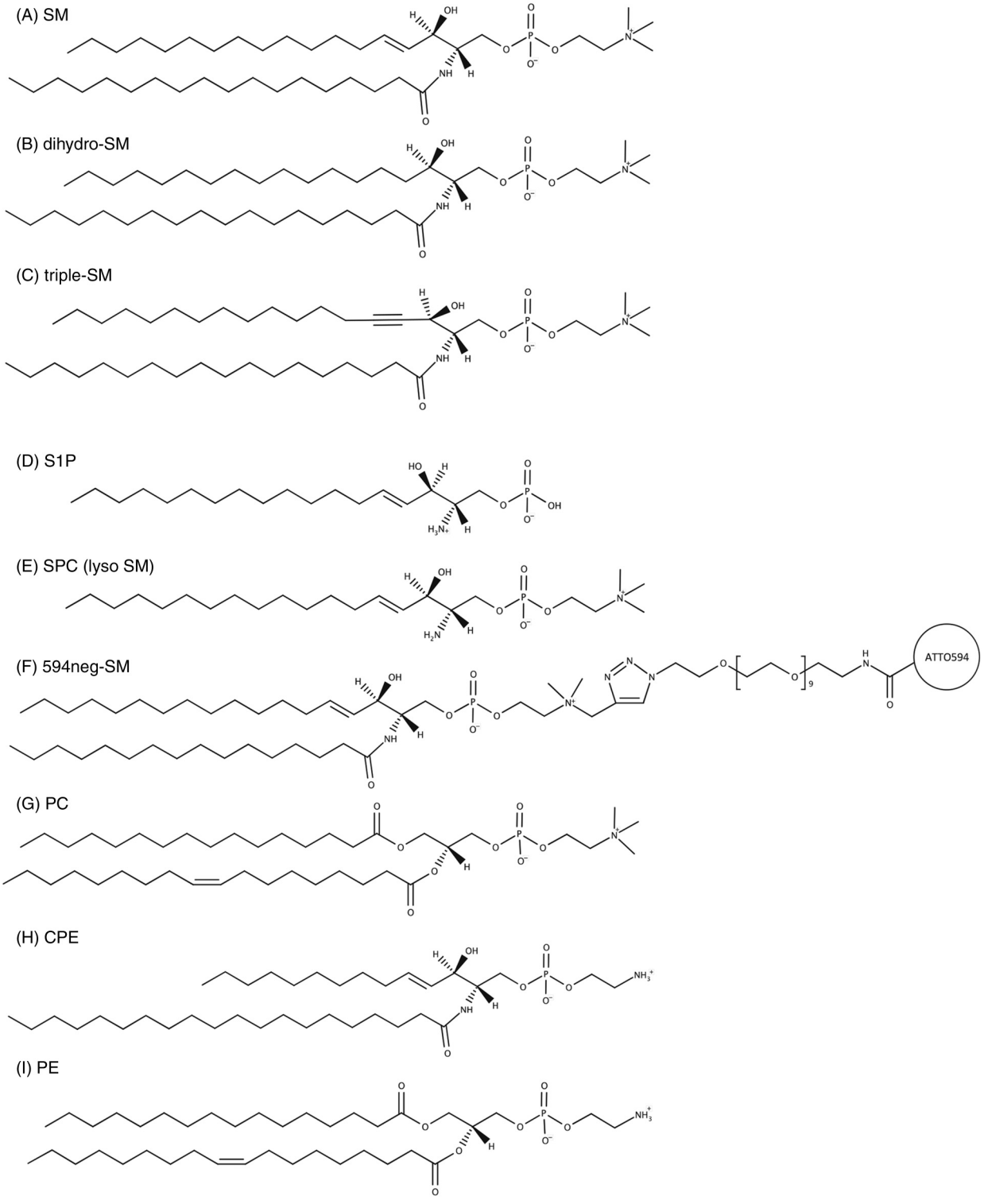

Figure 1. Structures of different lipids: (A) SM, (B) dihydro-SM, (C) triple-SM, (D) S1P, (E) SPC (lyso SM) (F) 594neg-SM, (G) PC, (H) CPE, and (I) PE.

SM = sphingomyelin; dihydro-SM = dihydrosphingomyelin; triple-SM = (2S,3S)-{2-[(2-hexadecanoylamino-3-hydroxyoctadec-4-ynyloxy)-hydroxyphosphoryloxy]ethyl}trimethylammonium; S1P = sphingosine-1-phosphate; SPC (lyso SM) = sphingosylphosphorylcholine; PC = phosphatidylcholine; CPE = ceramide phosphoethanolamine; PE = phosphatidylethanolamine.

These proteins revealed the detailed distribution of SM in the plasma membrane (Abe et al., 2012; Kiyokawa et al., 2005), the transbilayer asymmetry of SM (Murate et al., 2015), SM trafficking from the Golgi apparatus (Deng et al., 2016) and exposure of SM to the cytoplasmic leaflet of lysosomes under pathological conditions (Ellison et al., 2020). In these methods, SBPs labelled by fluorophores or fluorescent proteins were added to the medium to label cell surface SM in living cells. Alternatively, fluorescent protein-conjugated SBPs were expressed in the cytoplasma to label SM in the cytoplasmic leaflet of the plasma membrane and intracellular organelles. To observe SM in fixed cells by fluorescence or electron microscopy, cells were labelled with SBPs followed by fluorescent or immunogold-labelled antibodies. Thus, the results are primarily dependent on the SM–SBP interaction, which may be affected by different intrinsic and extrinsic factors. Understanding these factors is crucial to the utilization of SBPs to visualize cellular SM. Here, we summarize intrinsic and extrinsic factors affecting SBP binding to SM. Recent protocols (Abe & Kobayashi, 2021; Tomishige et al., 2021) are also helpful for SBPs utilization. The plasmids of SBPs developed by our group are available through the RIKEN BioResource Research Center DNA Bank (https://dna.brc.riken.jp/en/).

Intrinsic Factors Regulating the Lipid-Binding Specificity of SBPs

SM Reporters

Lysenin. Lysenin is an earthworm-derived 33-kDa pore-forming toxin (Shogomori & Kobayashi, 2008; Yamaji et al., 1998; Yamaji-Hasegawa et al., 2003; Yilmaz et al., 2013) that specifically binds SM ($K_D = 5.3 \times 10^{-9}$ M) (Yamaji et al., 1998). SM shares a phosphocholine head group with phosphatidylcholine (PC) (Figure 1G). However, enzyme-linked immunosorbent assay (ELISA) and thin-layer chromatography immunostaining assays indicated that lysenin bound SM but not PC (Yamaji et al., 1998). Lysenin also did not bind glycerophospholipids, ceramide, sphingosine, sphingosine-1-phosphate (S1P) (Figure 1D) or sphingosylphosphorylcholine (SPC, lyso SM) (Figure 1E) (Yamaji et al., 1998), suggesting that the ceramide-conjugated phosphocholine structure is recognized by lysenin. Lysenin bound dihydrosphingomyelin (dihydro-SM) (Figure 1B) and the SM analogue, (2S,3S)-{2-[(2-hexadecanoylamino-3-hydroxyoctadec-4-ynyloxy)-hydroxyphosphoryloxy]ethyl}trimethylammonium (triple-SM) (Figure 1C) (Kinoshita et al., 2013), suggesting that the double bond at the interfacial region of sphingosine in SM is not crucial for recognition by lysenin (Figure 2).

The crystal structure of lysenin revealed an N-terminal pore-forming module and a C-terminal beta-trefoil motif (De Colibus et al., 2012). Both modules contain SM or phosphocholine-binding sites. An N-terminal truncation mutant of lysenin retained specific binding to SM ($K_D = 1.9 \times 10^{-7}$ M) but was not toxic, suggesting that the C-terminal binding site is sufficient for SM binding. The shortest C-terminal fragment (amino acids 161–297) that binds SM was designated NT-Lys (Kiyokawa et al., 2005). Enhanced green fluorescent protein (EGFP)–NT-Lys bound SM but not SPC in ELISA (Makino et al., 2015). EGFP–NT-Lys also bound 594neg-SM, where ATTO594 dye is conjugated to propargyl-SM (Figure 1F) (Kinoshita et al., 2017), indicating that adding a fluorophore moiety to the headgroup of SM

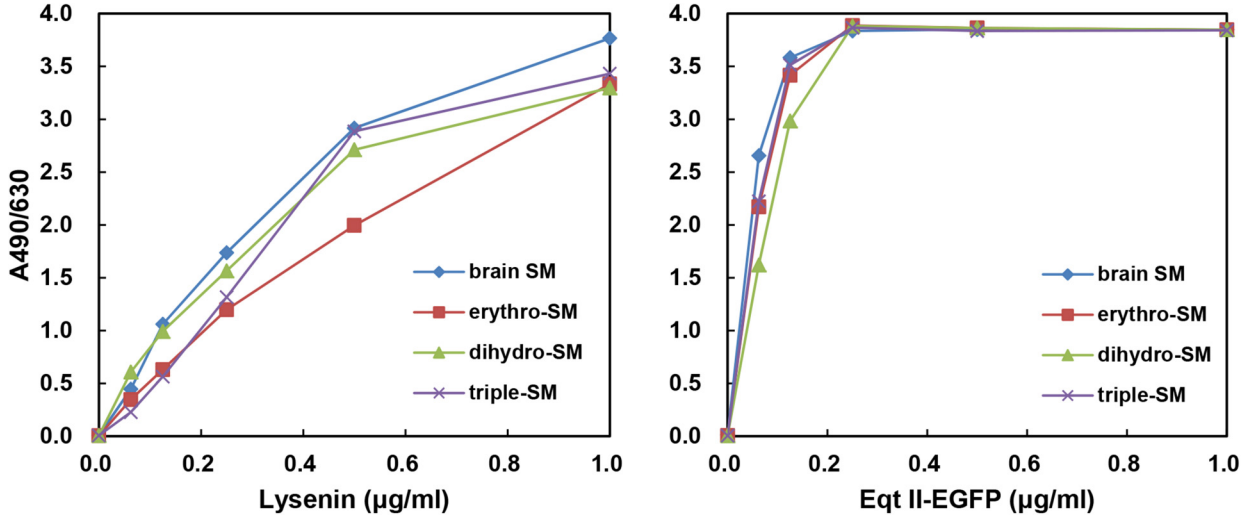

Figure 2. Binding of lysenin and EqtII–EGFP to SM, dihydro-SM and triple-SM. Binding of the proteins to the lipids was measured by ELISA as in Yamaji-Hasegawa et al. (2003).
EqtII = equinatoxin II; EGFP = enhanced green fluorescent protein; SM = sphingomyelin; dihydro-SM = dihydrosphingomyelin; triple-SM = (2S,3S)-{2-[(2-hexadecanoylamino-3-hydroxyoctadec-4-ynyloxy)-hydroxyphosphoryloxy]ethyl}trimethylammonium; ELISA = enzyme-linked immunosorbent assay.

does not inhibit lysenin binding. A variant with a single tryptophan to alanine mutation at position 20 of lysenin, W20A, was nontoxic and weakly bound SM when conjugated to maltose-binding protein (MBP) (Kiyokawa et al., 2004) or glutathione *S*-transferase (GST) (Kulma et al., 2010).

Fluorescent protein-conjugated lysenin (Canals et al., 2010; Ishitsuka et al., 2004; Kidani et al., 2012; Yachi et al., 2012), lysenin binding followed by anti-lysenin antibody detection (Kavishwar et al., 2011; Makino et al., 2015; Taksir et al., 2012; Yamaji et al., 1998) and recombinant MBP- or GST-lysenin binding followed by anti-MBP or anti-GST detection (Kiyokawa et al., 2004; Kulma et al., 2012; Makino et al., 2015; Nakai et al., 2000; Skocaj et al., 2014; Yoshida et al., 2001) have been used to localize SM in model membranes (Ishitsuka et al., 2004; Makino et al., 2015), in the plasma membrane of fixed cells (Canals et al., 2010; Kavishwar et al., 2011; Kidani et al., 2012; Kulma et al., 2012; Nakai et al., 2000; Skocaj et al., 2014), in the endocytic compartments of fixed and permeabilized cells (Kiyokawa et al., 2004; Yachi et al., 2012; Yamaji et al., 1998) and the sections of cells and organs (Makino et al., 2015; Taksir et al., 2012; Yoshida et al., 2001). However, the binding of lysenin at physiological temperature was followed by oligomerization of the protein and pore formation in the membrane, which is accompanied by reorganization of the membrane (Alam et al., 2012; Aoki et al., 2010; Bokori-Brown et al., 2016; Podobnik et al., 2016; Yamaji-Hasegawa et al., 2003; Yilmaz & Kobayashi, 2015; Yilmaz et al., 2013, 2018). Oligomerization of lysenin is temperature-dependent (Yamaji-Hasegawa et al., 2003). Ikenouchi et al. (2012, 2013) incubated paraformaldehyde-fixed cells with GFP- or monomeric red fluorescent protein-tagged lysenin on ice followed by fixation on ice to prevent lysenin oligomerization. Using this procedure, they showed selective labelling of the apical membranes of mouse mammary gland-derived epithelial cells with lysenin in a tight junction-independent manner (Ikenouchi et al., 2012) and the enrichment of SM clusters in microvilli (Ikenouchi et al., 2013). Full-length lysenin or MBP-lysenin was also used to label SM in sodium dodecyl sulphate-digested freeze fracture replica labelling, where lipids were physically fixed to a metal cast (Murate et al., 2015). Atomic force microscopy tips conjugated with lysenin were used to measure the binding force of SM and lysenin, and localize SM-rich domains in a supported bilayer (Dumitru et al., 2018; Wang et al., 2012).

Nonoligomerizable, nontoxic NT-Lys has been used to label both fixed and living cells (Abe et al., 2012; Carquin et al., 2014; Ellison et al., 2020; He et al., 2017; Kasahara et al., 2013; Kishimoto et al., 2020; Kiyokawa et al., 2005; Leonard et al., 2018; Makino et al., 2015; Mizuno et al., 2011; Mound et al., 2017). To study living cells, NT-Lys was labelled with a fluorophore or fluorescent protein conjugated to the N-terminus of NT-Lys. Fluorescent NT-Lys has been used to monitor the dynamics of SM accumulation in the cleavage furrow during cell division (Abe et al., 2012), SM redistribution during cell attachment (Kishimoto et al., 2020) and SM exposure to the cytoplasmic leaflet of endolysosomes after bacterial infection (Ellison et al., 2020) in living cells. Recently, Bhattacharya et al. (2021) reported a unique application of NT-Lys to monitor enzymatic in vitro synthesis of SM.

Equinatoxin II. Equinatoxin II (EqtII) is a sea anemone-derived 20-kDa pore-forming toxin belonging to the actinoporin family (Anderluh et al., 1996; Rojko et al., 2016). Specific binding of EqtII and EqtII–EGFP to SM ($K_D = 7.5 \times 10^{-9}$ M) (Hong et al., 2002) has been demonstrated by dot-blot (Bakrac et al., 2008), surface plasmon resonance (Bakrac et al., 2008) and ELISA (Makino et al., 2015). ELISA showed that EqtII–EGFP also binds SPC (Makino et al., 2015), dihydro-SM and triple-SM (Figure 2). The molecular mechanisms of pore formation by EqtII and another SM-binding actinoporin, sticholysin, have been extensively studied (Rivera-de-Torre et al., 2020; Rojko et al., 2016). Pore formation is a multiple-step process including binding to SM, an intramolecular conformational change in the protein, oligomerization on the membrane, and pore formation. Inhibition of the intramolecular conformational change by disulphide bridge formation in the double cysteine mutant EqtII(8–69) (V8C, K69C) prevented the haemolytic activity without perturbing SM-binding activity under oxidized conditions (Hong et al., 2002; Kristan et al., 2004; Rojko et al., 2013). Similar to EqtII–EGFP, EqtII(8–69)–EGFP bound SM and SPC, but not glycerophospholipids

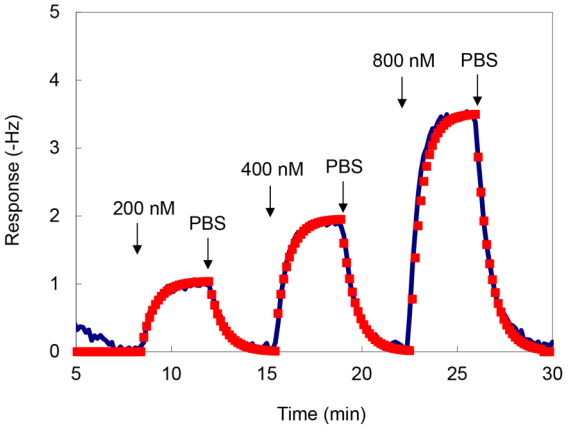

Figure 3. QCM sensorgram of the binding of nakanori to equimolar CPE/Chol membranes. Quartz crystal microbalance with dissipation monitoring (QCM-D) measurement was performed according to a published method (Bhat et al., 2015). The indicated concentrations of recombinant protein and PBS were added stepwise while ΔF was measured (red) and the dissociation constant (K_D) of nakanori was estimated from the fitting curves of the association and dissociation (blue).
QCM = quartz crystal microbalance; CPE = ceramide phosphoethanolamine; Chol = cholesterol; PBS = phosphate-buffered saline.

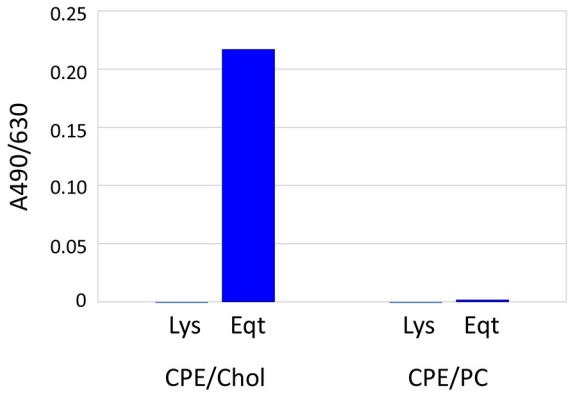

Figure 4. Binding of EGFP–NT-Lys and EqtII–EGFP to CPE/Chol and CPE/PC. Binding of the proteins to the lipids was measured by ELISA as in Yamaji-Hasegawa et al. (2003).
EGFP = enhanced green fluorescent protein; EqtII = equinatoxin II; CPE = ceramide phosphoethanolamine; Chol = cholesterol; PC = phosphatidylcholine; ELISA = enzyme-linked immunosorbent assay.

and glycosphingolipids (GSLs) by ELISA (Makino et al., 2015). Since the nontoxic property of EqtII(8–69) is dependent on the oxidative environment, application of this protein in the intracellular reduced condition is difficult. Recently, a nontoxic double mutant of EqtII, Eqt(V22W, Y108I) was reported (Deng et al., 2016). This protein was bound to the cell surface and the labelling was abolished by SM removal by sphingomyelinase (SMase). This protein was used to follow the release of SM-containing vesicles from the *trans*-Golgi network and SM transport to the plasma membrane in living cells (Deng et al., 2016).

SM/Chol Reporters

Aegerolysins. Mushroom-derived aegerolysin proteins are ~15-kDa membrane-binding components of two-component pore-forming toxins (Butala et al., 2017). The binding of aegerolysins to the target membrane is followed by the recruitment of pore-forming subunits, oligomerization of the protein complex, and pore formation. However, aegerolysins themselves are nontoxic, although a high concentration of ostreolysin A (OlyA) induces plasma membrane shedding (Skocaj et al., 2016). Screening of SM/Chol-binding proteins from the extract of the mushroom *Pleurotus eryngii* identified the aegerolysin family protein, pleurotolysin A2 (PlyA2) (Bhat et al., 2013). PlyA2 is 80% identical to OlyA. C-terminally EGFP-tagged PlyA2 (PlyA2-EGFP) but not N-terminally tagged protein (EGFP-PlyA2) also bound SM/Chol but not GSL/Chol. Examining different sterols revealed the importance of the stereoconfiguration of the 3-hydroxyl group of sterol for binding (Bhat et al., 2013). PlyA2-EGFP labelled plasma membrane and late endosomes of HeLa cells. This binding was abolished by pretreatment of cells with SMase to remove SM or methyl-β-cyclodextrin to remove Chol (Bhat et al., 2013). Similar to PlyA2-EGFP, OlyA-mCherry bound SM/Chol and labelled living and fixed cells in an SM- and a Chol-dependent manner (Skocaj et al., 2014). The conformation of SM is speculated to be altered by the presence of Chol (Endapally et al., 2019). Aegerolysins recognize only Chol-bound conformations whereas lysenin and EqtII bind both Chol-bound and Chol-free conformations. Biochemical and structural analyses revealed that a single glutamic acid residue of OlyA is involved in the selective recognition of the Chol-bound conformation of SM (Endapally et al., 2019). Despite its specificity, the affinity of PlyA2-EGFP and OlyA-EGFP to SM/Chol was too weak to measure K_D by quartz crystal microbalance with dissipation monitoring (QCM-D) (Bhat et al., 2015). Erylysin A (EryA) is 98% homologous to PlyA2, but EryA-EGFP does not bind SM/Chol or SM (Bhat et al., 2015; Panevska et al., 2019a). The lipid specificity of SM/Chol reporters was recently summarized (Grundner et al., 2021).

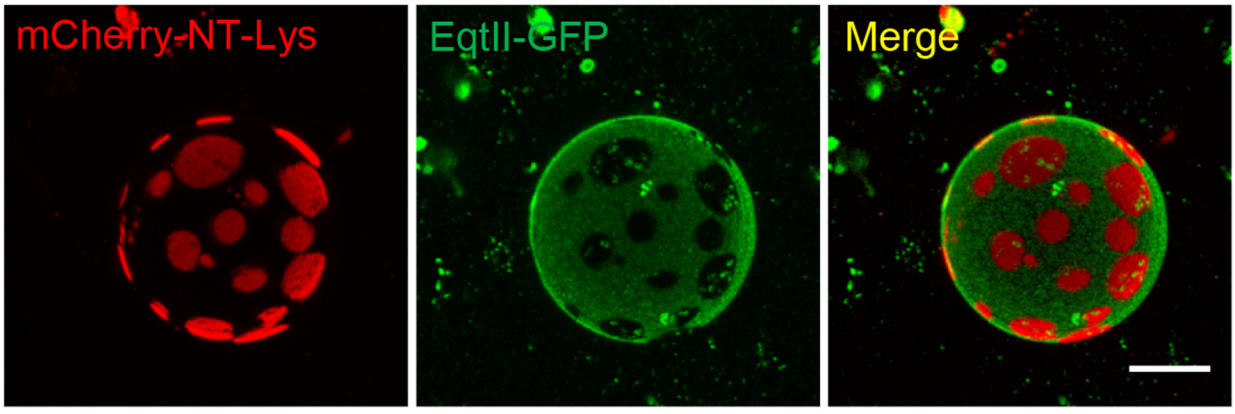

Figure 5. Binding of mCherry–NT-Lys and EqtII–GFP to GUVs composed of eSM/diC18:1PC/Chol (2:2:1). Fluorescence images displaying exclusive labelling were obtained by confocal microscopy. Scale bar =20 μm. Adapted from Makino et al. (2015).
EqtII = equinatoxin II; GFP = green fluorescent protein; GUV = giant unilamellar vesicle; eSM = egg sphingomyelin; diC18:1PC = dioleoyl phosphatidylcholine; Chol = cholesterol.

Nakanori. Nakanori (mid-raft rider in Japanese) is an additional SM/Chol-binding protein from the edible mushroom *Grifola frondosa* (Makino et al., 2017). Nakanori shows no sequence homology with other SM- or SM/Chol-binding proteins. However, the crystal structure of nakanori overlaps with that of the SM-binding toxin, sticholysin, with an extra N-terminus (Makino et al., 2017). Unlike sticholysin, nakanori was not toxic, perhaps because the extra N-terminus may inhibit oligomerization and pore formation. In contrast to aegerolysins, nakanori showed high affinity ($K_D = 1.4 \times 10^{-7}$ M) to the SM/Chol membrane (Makino et al., 2017). Nakanori did not bind glycerolipids/Chol and GSL/Chol. More than 30 mol% Chol was required for binding to SM/Chol-containing membranes. Binding experiments of nakanori to SM/PC/Chol liposomes with different PC contents suggested that nakanori bound pre-existing SM/Chol domains and was not able to induce the formation of SM/Chol complexes (Makino et al., 2017). Nakanori identified SM/Chol-rich lipid domains on the cell surface and in intracellular membranes. Nakanori was also applied to follow the dynamics of SM/Chol domains on the cell surface by single-molecule tracking (Makino et al., 2017).

Ceramide Phosphoethanolamine (CPE) Reporters

Very weak binding of aegerolysins to SM/Chol led to the screening of the high-affinity lipid ligands of proteins. Screening identified CPE as a high-affinity ligand. CPE is

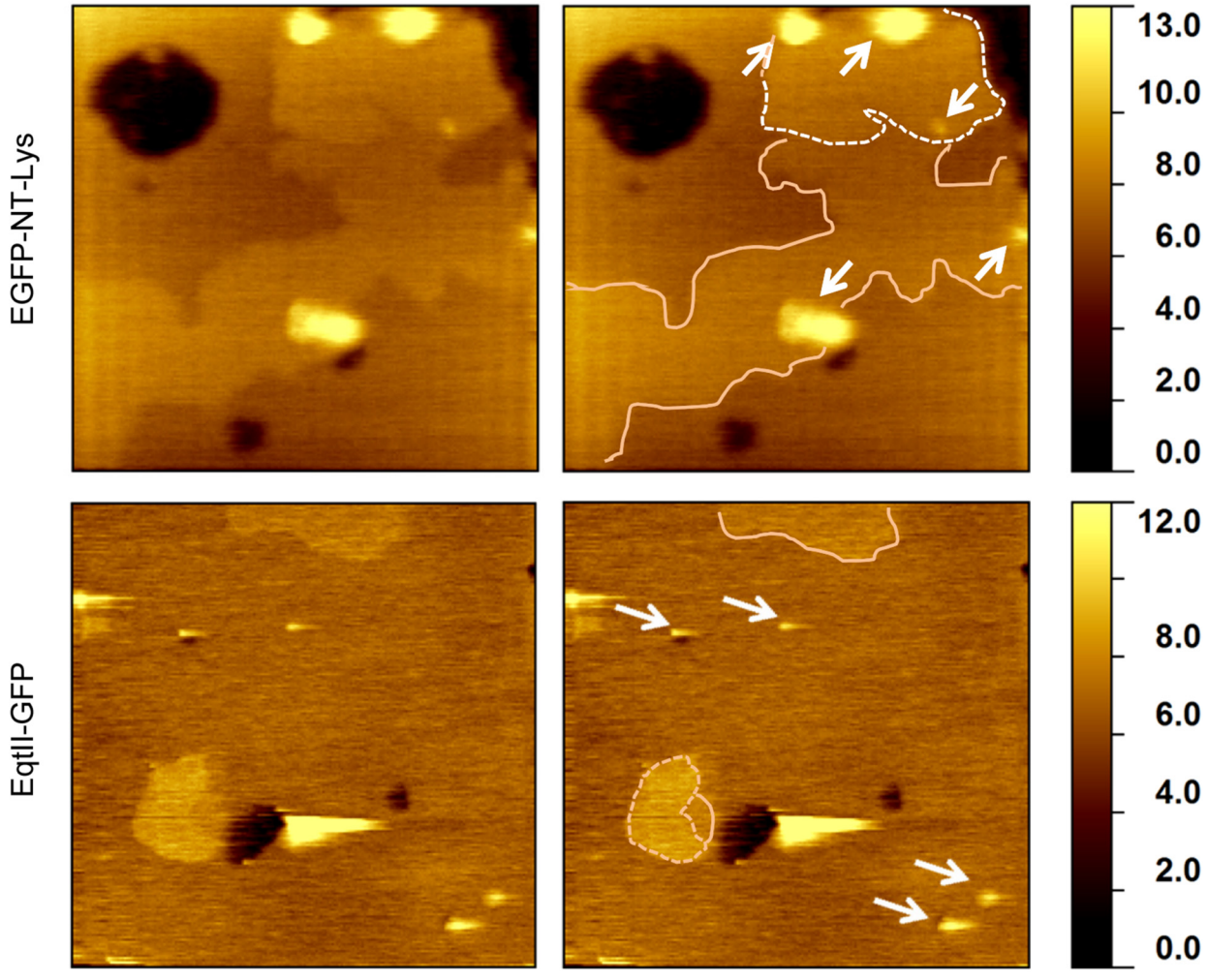

Figure 6. Atomic force microscopy images of EGFP–NT-Lys and EqtII–GFP bound to different regions of the eSM/diC18:1PC bilayer. The scale bars next to each image indicate the height (nanometres). The scan sizes of images from top to bottom are 400 × 400 nm and 1 × 1 μm, respectively. The eSM/diC18:1PC bilayer separated into three phases: eSM-rich, eSM/diC18:1PC-mixed, and diC18:1PC-rich phases. On the images to the right, the borders of eSM-rich and eSM/diC18:1PC-mixed domains are indicated by dashed and solid lines, respectively. The white arrows point to the proteins. Adapted from Makino et al. (2015).
EGFP = enhanced green fluorescent protein; EqtII = equinatoxin II; GFP = green fluorescent protein; eSM = egg sphingomyelin; diC18:1PC = dioleoyl phosphatidylcholine.

an analogue of SM in which the phosphocholine moiety of SM is replaced with phosphoethanolamine (Murate et al., 2020; Panevska et al., 2019b) (Figure 1H). CPE is a major sphingolipid in insects and parasites but exists only in trace amounts in mammalian cells. The K_D values of PlyA2-EGFP, OlyA-EGFP and EryA-EGFP to CPE/Chol (1:1) were 1.2×10^{-8}, 1.2×10^{-9} and 1.3×10^{-9} M, respectively (Bhat et al., 2015). PlyA2 also weakly bound CPE in the absence of Chol ($K_D = 4.1 \times 10^{-5}$ M) (Bhat et al., 2015). Similar to PlyA2-EGFP-binding to SM/sterol, the binding of OlyA-EGFP to CPE/sterol was dependent on the 3-hydroxyl group of sterol (Bhat et al., 2015). Phosphatidylethanolamine (PE) (Figure 1I) shares a small headgroup with CPE. However, aegerolysins did not bind PE/Chol (Bhat et al., 2015). PlyA2-EGFP revealed the enrichment of CPE in the central nervous system of *Drosophila* larvae and the EryA-EGFP stage-specifically labelled parasite *Trypanosoma brucei* (Bhat et al., 2015). PlyA2, OlyA and EryA showed selective toxicity towards western corn rootworm larvae and adults, and Colorado potato beetle larvae when mixed with pore-forming subunit PlyB (Panevska et al., 2019a). The W6A mutant of PlyA2-His inhibited the binding of the protein to CPE/PC but not SM/Chol and CPE/Chol. In contrast, the W28A mutant inhibited binding to SM/Chol but not CPE/PC (Bhat et al., 2015). Although the binding of PlyA2-EGFP to HeLa cells was completely inhibited by preincubation of the protein with SM/Chol liposomes, the binding was partially inhibited by CPE/Chol and was not affected by CPE/PC (Bhat et al., 2015). These results suggest that the binding site of PlyA2 to SM and CPE may be different. Similar to aegerolysins, nakanori bound CPE/Chol (Figure 3). However, the K_D to CPE/Chol (1.9×10^{-6} M) was 100 to 1,000 times higher than those of aegerolysins. EqtII–EGFP but not EGFP–NT-Lys also bound CPE/Chol (Figure 4), which is interesting when we consider the physiological target of EqtII since CPE is widely distributed in Mollusca (Panevska et al., 2019b) who eats sea anemone, a producer of EqtII.

Extrinsic Factors: Effect of Phase and Lipid Density

Lysenin bound both the gel state {stearoyl SM (C18:0 SM, gel to liquid crystalline phase transition temperature, T_m, at 52.8° C [Bunow, 1979])} and liquid crystalline state {oleoyl SM (C18:1 SM, T_m at 33.0°C [Ahmad et al., 1985])} at 37°C (Yamaji-Hasegawa et al., 2003), suggesting that the phase state of SM does not affect lysenin binding. However, lysenin bound egg SM {eSM, a major component is palmitoyl SM (C16:0 SM, T_m at 41°C [Marsh, 2013])} in dioleoyl PC (diC18:1 PC, T_m at −20°C [Marsh, 2013]) but not in dipalmitoyl PC (diC16:0 PC, T_m at 41°C [Marsh, 2013]) (Ishitsuka et al., 2004; Makino et al., 2015). The stoichiometry of SM/lysenin was calculated to be 5 to 6 by isothermal calorimetry (ITC) (Ishitsuka & Kobayashi, 2007; Ishitsuka et al., 2004). In diC18:1 PC, SM is speculated to form clusters of >5 to 6 molecules. However, in diC16:0 PC, mixing C16:0 PC and SM hinders the formation of SM clusters (Ishitsuka et al., 2004; Makino et al., 2015). Most GSLs have high T_m. Similar to diC16:0 PC, GSLs inhibited lysenin binding to SM both in

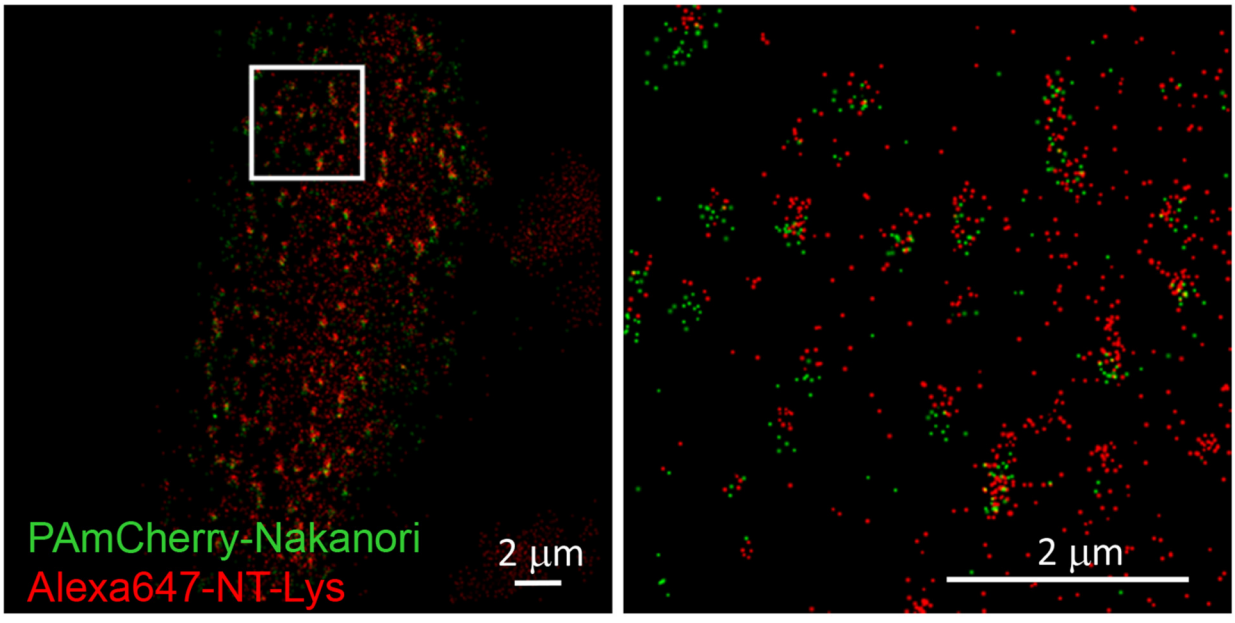

Figure 7. PALM/dSTORM images of HeLa cells doubly labelled with pAmCherry-nakanori (green) and Alexa647–NT-Lys (red). The boxed area in the left panel is enlarged in the right panel. Adapted from Makino et al. (2017).
PALM = photo-activated localization microscopy; dSTORM = direct stochastic optical reconstitution microscopy.

model and cell membranes (Ishitsuka et al., 2004; Kiyokawa et al., 2005; Makino et al., 2015).

In phase-separated eSM/diC18:1 PC/Chol giant unilamellar vesicles (GUVs), mCherry–NT-Lys bound exclusively liquid-ordered domains, whereas EqtII–EGFP selectively bound disordered domains (Figure 5) (Makino et al., 2015). Atomic force microscopy showed that in SM/diC18:1 PC supported bilayer, EGFP–NT-Lys bound SM-rich lipid domains, whereas EqtII–GFP bound SM-poor, diC18:1 PC-rich lipid domains (Figure 6) (Makino et al., 2015). Preferential partitioning of EqtII to the liquid disordered phase was also shown using phase-separated droplet interface bilayers (Rojko et al., 2014). However, in contrast to lysenin, EqtII bound a solid eSM/diC16:0 PC membrane (Makino et al., 2015). EqtII is speculated to bind SM when the density of lipids in the membrane is low. Clustering of SM may inhibit the binding of EqtII (Makino et al., 2015).

The binding of PlyA2, OlyA and nakanori required a high membrane concentration (>30%) of Chol. Thus, these proteins selectively bound liquid-ordered SM/Chol lipid domains. Super-resolution microscopy indicated that nakanori-positive SM/Chol-rich domains were part of the SM-rich domains labelled with NT-Lys (Figure 7).

Conclusion and Perspectives

Table 1 summarizes the binding specificity of different SBPs and Figure 8 schematically shows the binding of different

Table 1. Lipid Specificity of Sphingomyelin-Binding Proteins.

	Lysenin	EGFP–NT-Lys	EqtII–EGFP	PlyA2–EGFP	Aegerolysins OlyA–EGFP	EryA–EGFP	Nakanori
bSM	+++[a]	+++[b]	+++[c]	−[d]			−[e]
16:0SM	+++[f]	+++[c]	+++[c]				
18:0SM	+++[f,g]		+++[g]				
Dihydro-18:0SM	+++[g]		+++[g]				
Triple-18:0SM	+++[g]		+++[g]				
SPC	−[f]	−[c]	++[c]				
594neg-SM		++[h]					
PC	−[a]	−[c]	−[c]	−[i]	−[i]	−[i]	−[j]
SM/Chol	+++[k]			+[l]	+[l]	−[l]	+++[m]
16:0SM/diC18:1PC	+++[n]	+++[o]	+++[o]				
16:0SM/diC16:0PC	−[n]	±[o]	+++[o]				
SM/GSL	−[p]	−[q]	+++[q]				
CPE/Chol		−[g]	++[g]	+++[r]	+++[r]	+++[r]	++[s]
CPE/PC		−[g]	−[g]	++[p]	−[l]	−[l]	
PE/Chol				−[l]	−[l]	−[l]	
PE	−[a]	−[c]	−[c]				

bSM = brain sphingomyelin; 16:0SM = palmitoyl SM; 18:0SM = stearoyl SM; SPC = sphingosylphosphorylcholine (lyso SM); 594neg-SM = ATTO594-propargyl-SM; PC = phosphatidylcholine; Chol = cholesterol; diC18:1PC = dioleoyl phosphatidylcholine; diC16:0PC = dipalmitoyl phosphatidylcholine; GSL = glycosphingolipid; CPE = ceramide phosphoethanolamine; PE = phosphatidylethanolamine; ELISA = enzyme-linked immunosorbent assay; ITC = isothermal calorimetry; QCM-D = quartz crystal microbalance with dissipation monitoring; OlyA = ostreolysin A; PlyA2 = pleurotolysin A2; EryA = erylysin A.

[a] ELISA, dot-blot, liposome lysis (Yamaji et al., 1998).
[b] ELISA (His-Venus-NT-Lys and His-monomeric Venus-NT-Lys) (Kiyokawa et al., 2005).
[c] ELISA (Makino et al., 2015).
[d] Binding to SM/C16:0–C18:1PC (1:1) liposomes (Bhat et al., 2013).
[e] ELISA (Makino et al., 2017).
[f] ELISA (Yamaji-Hasegawa et al., 2003).
[g] ELISA, this study (Figures 2 and 4).
[h] ELISA (Kinoshita et al., 2017).
[i] Binding to PC/Chol (1:1) liposomes (Bhat et al., 2015).
[j] ELISA, liposome binding and ITC using PC/Chol (1:1) (Makino et al., 2017).
[k] Liposome binding and ITC (Ishitsuka & Kobayashi, 2007).
[l] Liposome binding (Bhat et al., 2015).
[m] ELISA, liposome binding. ITC and QCM-D (Makino et al., 2017).
[n] Liposome binding (Ishitsuka et al., 2004).
[o] ELISA and liposome binding (Makino et al., 2015).
[p] Binding to lipid monolayer and liposomes, labelling of control and GSL-deficient melanoma cells (Ishitsuka et al., 2004).
[q] Labelling of control and GSL-deficient melanoma cells (Makino et al., 2015).
[r] Liposome binding, QCM-D (Bhat et al., 2015).
[s] QCM-D, this study (Figure 3).

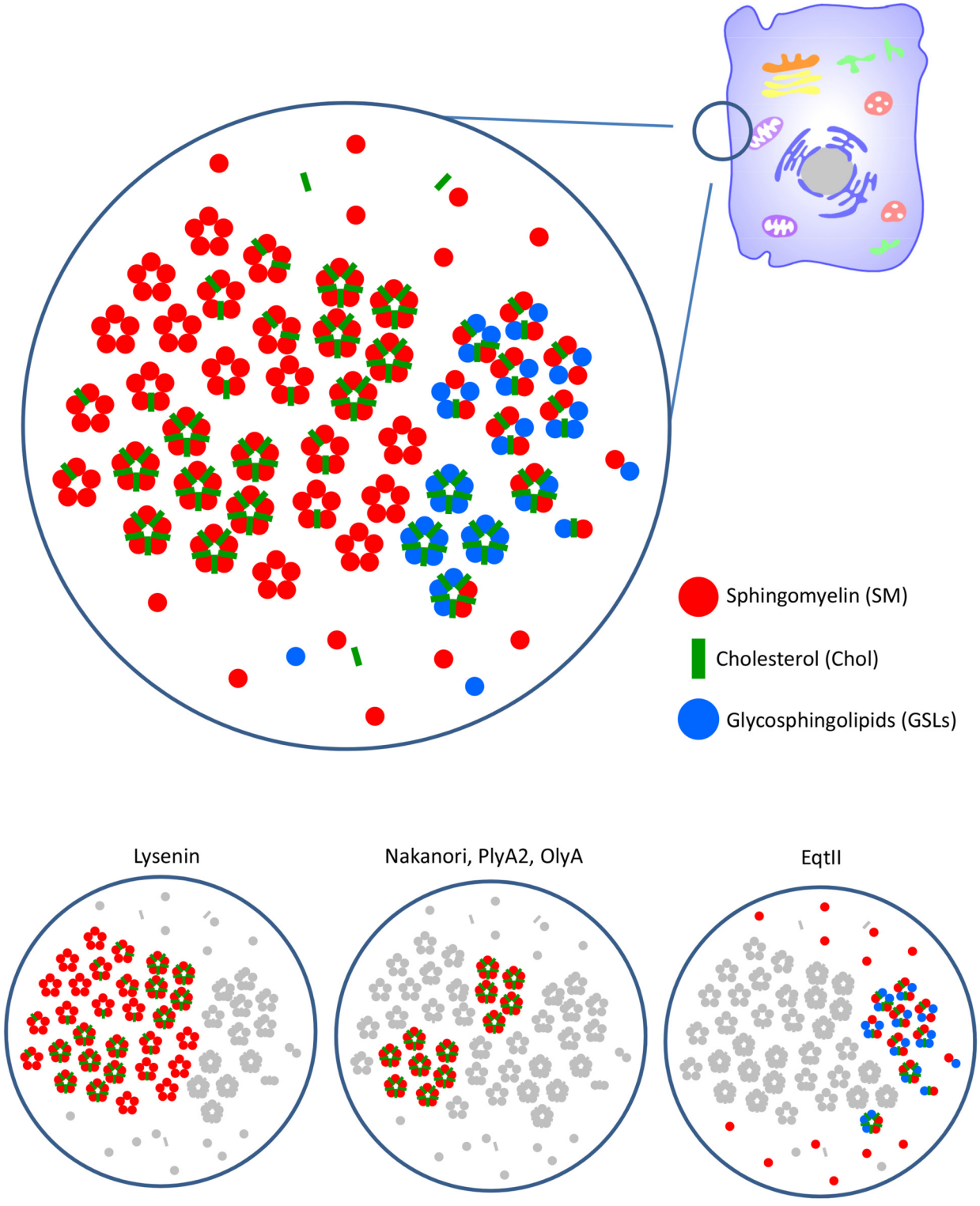

Figure 8. Speculative distribution of plasma membrane SM and other lipids detected by SBPs. SM forms lipid clusters with Chol and GSLs with different stoichiometries. Alternatively, SM distributes as a monomer in the glycerolipid-rich membrane. Glycerolipids are not shown in the model. Lysenin preferentially binds clusters of 5 to 6 SM molecules. Chol does not affect lysenin binding. Lysenin does not bind when SM forms a co-cluster with GSLs. Nakanori, PlyA2, and OlyA bind the SM/Chol clusters when the Chol/SM ratio is higher than 30%. EqtII does not bind SM clusters. EqtII labels the SM monomer and SM co-clustered with GSLs.
SM = sphingomyelin; SBP = SM-binding protein; Chol = cholesterol; GSL = glycosphingolipid; EqtII = equinatoxin II; OlyA = ostreolysin A; PlyA2 = pleurotolysin A2.

SBPs to various lipid domains. SM is speculated to form clusters with GSLs, Chol and other SM molecules through the hydrophobic interaction of the saturated acyl moiety and hydrogen bonds. Thus, different clusters composed of SM, SM/Chol, SM/GSL and SM/GSL/Chol with different stoichiometries may exist in the plasma membrane. In addition, SM monomers may be located in the glycerophospholipid-rich areas (Figure 8). Lysenin and NT-Lys bind SM and SM/Chol clusters but not SM/GSL clusters. In contrast to lysenin, EqtII binds SM/GSL clusters. Aegerolysins and nakanori selectively label SM/Chol clusters. SM/Chol clusters form domains belonging to the lysenin-labelled domains of SM clusters (Figure 7). Thus, each SBP highlights specific SM pools. Previously, different SBPs revealed alterations in SM distributions in pathological conditions (Makino et al., 2015, 2017).

In the cell membranes, SM rapidly diffuses laterally and moves from one membrane to another during endocytosis or budding. The binding of SBPs may partially inhibit SM dynamics. Indeed, the binding of OlyA changed the cell surface Chol pool and disrupted intracellular trafficking of Chol (Johnson et al., 2019). Inhibition of lipid dynamics by high concentrations of SBPs may explain membrane shedding induced by OlyA (Skocaj et al., 2016) and the influenza virus budding inhibition by nakanori (Makino et al., 2017). Thus, interpretation of the use of SBPs in live cell assays needs to be accompanied with some caution.

The distribution and dynamics of SM and SM/Chol-rich lipid domains remain controversial. Considering their precise binding specificity and potential drawbacks, SBPs appear to be useful tools, when combined with biochemical and biophysical analyses, to study the distribution, dynamics, and function of SM.

Acknowledgments

We are grateful to Brigitte Pollet for her technical assistance.

Declaration of Conflicting Interests

The authors declared no potential conflicts of interest with respect to the research, authorship, and/or publication of this article.

Funding

The authors disclosed receipt of the following financial support for the research, authorship, and/or publication of this article: Grants-in-Aid from the Ministry of Education, Culture, Sports, Science, and Technology of Japan (25293015 to T.K.), Agence Nationale pour la Recherche (A20R417C to T.K.), Agence Nationale de Recherche sur le Sida et les Hépatites virale (18365 to T.K.), Ligue Contre le Cancer (to T.K.), Vaincre les Maladies Lysosomales (19/LBPH/S44 to T.K.), Eucor seed money grant, RIKEN Integrated Lipidology Program and RIKEN Glyco-lipidologue Program (to T.K.).

ORCID iD

Toshihide Kobayashi https://orcid.org/0000-0002-4811-7270

References

Abe, M., & Kobayashi, T. (2021). Imaging sphingomyelin- and cholesterol-enriched domains in the plasma membrane using a novel probe and super-resolution microscopy. *Advances in Experimental Medicine and Biology*, *1310*, 81–90. https://doi.org/10.1007/978-981-33-6064-8_4

Abe, M., Makino, A., Hullin-Matsuda, F., Kamijo, K., Ohno-Iwashita, Y., Hanada, K., Mizuno, H., Miyawaki, A., & Kobayashi, T. (2012). A role for sphingomyelin-rich lipid domains in the accumulation of phosphatidylinositol 4,5-bisphosphate to the cleavage furrow during cytokinesis. *Molecular and Cellular Biology*, *32*, 1396–1407. https://doi.org/10.1128/MCB.06113-11

Ahmad, T. Y., Sparrow, J. T., & Morrisett, J. D. (1985). Fluorine-, pyrene-, and nitroxide-labeled sphingomyelin: Semi-synthesis and thermotropic properties. *Journal of Lipid Research*, *26*, 1160–1165. https://doi.org/10.1016/S0022-2275(20)34290-5

Alam, J. M., Kobayashi, T., & Yamazaki, M. (2012). The single-giant unilamellar vesicle method reveals lysenin-induced pore formation in lipid membranes containing sphingomyelin. *Biochemistry*, *51*, 5160–5172. https://doi.org/10.1021/bi300448g

Anderluh, G., Pungercar, J., Strukelj, B., Macek, P., & Gubensek, F. (1996). Cloning, sequencing, and expression of equinatoxin II. *Biochemical and Biophysical Research Communications*, *220*, 437–442. https://doi.org/10.1006/bbrc.1996.0391

Aoki, T., Hirano, M., Takeuchi, Y., Kobayashi, T., Yanagida, T., & Ide, T. (2010). Single channel properties of lysenin measured in artificial lipid bilayers and their applications to biomolecule detection. *Proceedings of the Japan Academy*, *86*, 920–925. https://doi.org/10.2183/pjab.86.920

Bakrac, B., Gutierrez-Aguirre, I., Podlesek, Z., Sonnen, A. F., Gilbert, R. J., Macek, P., Lakey, J. H., & Anderluh, G. (2008). Molecular determinants of sphingomyelin specificity of a eukaryotic pore-forming toxin. *Journal of Biological Chemistry*, *283*, 18665–18677. https://doi.org/10.1074/jbc.M708747200

Bakrac, B., Kladnik, A., Macek, P., McHaffie, G., Werner, A., Lakey, J. H., & Anderluh, G. (2010). A toxin-based probe reveals cytoplasmic exposure of Golgi sphingomyelin. *Journal of Biological Chemistry*, *285*, 22186–22195. https://doi.org/10.1074/jbc.M110.105122

Bhat, H. B., Ishitsuka, R., Inaba, T., Murate, M., Abe, M., Makino, A., Kohyama-Koganeya, A., Nagao, K., Kurahashi, A., Kishimoto, T., Tahara, M., Yamano, A., Nagamune, K., Hirabayashi, Y., Juni, N., Umeda, M., Fujimori, F., Nishibori, K., & Yamaji-Hasegawa, A.,…, & Kobayashi, T. (2015). Evaluation of aegerolysins as novel tools to detect and visualize ceramide phosphoethanolamine, a major sphingolipid in invertebrates. *FASEB Journal*, *29*, 3920–3934. https://doi.org/10.1096/fj.15-272112

Bhat, H. B., Kishimoto, T., Abe, M., Makino, A., Inaba, T., Murate, M., Dohmae, N., Kurahashi, A., Nishibori, K., Fujimori, F., Greimel, P., Ishitsuka, R., & Kobayashi, T. (2013). Binding of a pleurotolysin ortholog from Pleurotus eryngii to sphingomyelin and cholesterol-rich membrane domains. *Journal of Lipid Research*, *54*, 2933–2943. https://doi.org/10.1194/jlr.D041731

Bhattacharya, A., Cho, C. J., Brea, R. J., & Devaraj, N. K. (2021). Expression of fatty acyl-CoA ligase drives one-pot de novo synthesis of membrane-bound vesicles in a cell-free transcription-

translation system. *Journal of the American Chemical Society*, *143*, 11235–11242. https://doi.org/10.1021/jacs.1c05394.

Bokori-Brown, M., Martin, T. G., Naylor, C. E., Basak, A. K., Titball, R. W., & Savva, C. G. (2016). Cryo-EM structure of lysenin pore elucidates membrane insertion by an aerolysin family protein. *Nature Communications*, *7*, 11293. https://doi.org/10.1038/ncomms11293

Bunow, M. R. (1979). Two gel states of cerebrosides. Calorimetric and Raman spectroscopic evidence. *Biochimica et Biophysica Acta*, *574*, 542–546. https://doi.org/10.1016/0005-2760(79)90250-9

Butala, M., Novak, M., Krasevec, N., Skocaj, M., Veranic, P., Macek, P., & Sepcic, K. (2017). Aegerolysins: Lipid-binding proteins with versatile functions. *Seminars in Cell and Developmental Biology*, *72*, 142–151. https://doi.org/10.1016/j.semcdb.2017.05.002

Canals, D., Jenkins, R. W., Roddy, P., Hernandez-Corbacho, M. J., Obeid, L. M., & Hannun, Y. A. (2010). Differential effects of ceramide and sphingosine-1-phosphate on ERM phosphorylation: Probing sphingolipid signaling at the outer plasma membrane. *Journal of Biological Chemistry*, *285*, 32476–32485. https://doi.org/10.1074/jbc.M110.141028

Carquin, M., Pollet, H., Veiga-da-Cunha, M., Cominelli, A., Van Der Smissen, P., N'Kuli, F., Emonard, H., Henriet, P., Mizuno, H., Courtoy, P. J., & Tyteca, D. (2014). Endogenous sphingomyelin segregates into submicrometric domains in the living erythrocyte membrane. *Journal of Lipid Research*, *55*, 1331–1342. https://doi.org/10.1194/jlr.M048538

De Colibus, L., Sonnen, A. F., Morris, K. J., Siebert, C. A., Abrusci, P., Plitzko, J., Hodnik, V., Leippe, M., Volpi, E., Anderluh, G., & Gilbert, R. J. (2012). Structures of lysenin reveal a shared evolutionary origin for pore-forming proteins and its mode of sphingomyelin recognition. *Structure (London, England: 1993)*, *20*, 1498–1507. https://doi.org/10.1016/j.str.2012.06.011

Deng, Y., Rivera-Molina, F. E., Toomre, D. K., & Burd, C. G. (2016). Sphingomyelin is sorted at the trans Golgi network into a distinct class of secretory vesicle. *Proceedings of the National Academy of Sciences of the USA*, *113*, 6677–6682. https://doi.org/10.1073/pnas.1602875113

Dumitru, A. C., Conrard, L., Lo Giudice, C., Henriet, P., Veiga-da-Cunha, M., Derclaye, S., Tyteca, D., & Alsteens, D. (2018). High-resolution mapping and recognition of lipid domains using AFM with toxin-derivatized probes. *Chemical Communication*, *54*, 6903–6906. https://doi.org/10.1039/C8CC02201A

Ellison, C. J., Kukulski, W., Boyle, K. B., Munro, S., & Randow, F. (2020). Transbilayer movement of sphingomyelin precedes catastrophic breakage of enterobacteria-containing vacuoles. *Current Biology*., *30*, 2974–2983, e2976. https://doi.org/10.1016/j.cub.2020.05.083

Endapally, S., Frias, D., Grzemska, M., Gay, A., Tomchick, D. R., & Radhakrishnan, A. (2019). Molecular discrimination between Two conformations of sphingomyelin in plasma membranes. *Cell*, *176*, 1040–1053, e1017. https://doi.org/10.1016/j.cell.2018.12.042

Grundner, M., Panevska, A., Sepcic, K., & Skocaj, M. (2021). What can mushroom proteins teach us about lipid rafts? *Membranes*, *11*, 264. https://doi.org/10.3390/membranes11040264

He, C., Hu, X., Jung, R. S., Weston, T. A., Sandoval, N. P., Tontonoz, P., Kilburn, M. R., Fong, L. G., Young, S. G., & Jiang, H. (2017). High-resolution imaging and quantification of plasma membrane cholesterol by NanoSIMS. *Proceedings of the National Academy of Sciences of the USA*, *114*, 2000–2005. https://doi.org/10.1073/pnas.1621432114

Hong, Q., Gutierrez-Aguirre, I., Barlic, A., Malovrh, P., Kristan, K., Podlesek, Z., Macek, P., Turk, D., Gonzalez-Manas, J. M., Lakey, J. H., & Anderluh, G. (2002). Two-step membrane binding by equinatoxin II, a pore-forming toxin from the sea anemone, involves an exposed aromatic cluster and a flexible helix. *Journal of Biological Chemistry*, *277*, 41916–41924. https://doi.org/10.1074/jbc.M204625200

Ikenouchi, J., Hirata, M., Yonemura, S., & Umeda, M. (2013). Sphingomyelin clustering is essential for the formation of microvilli. *Journal of Cell Science*, *126*, 3583–3592. https://doi.org/10.1242/jcs.122325

Ikenouchi, J., Suzuki, M., Umeda, K., Ikeda, K., Taguchi, R., Kobayashi, T., Sato, S. B., Kobayashi, T., Stolz, D. B., & Umeda, M. (2012). Lipid polarity is maintained in absence of tight junctions. *Journal of Biological Chemistry*, *287*, 9525–9533. https://doi.org/10.1074/jbc.M111.327064

Ishitsuka, R., & Kobayashi, T. (2007). Cholesterol and lipid/protein ratio control the oligomerization of a sphingomyelin-specific toxin, lysenin. *Biochemistry*, *46*, 1495–1502. https://doi.org/10.1021/bi061290k

Ishitsuka, R., Yamaji-Hasegawa, A., Makino, A., Hirabayashi, Y., & Kobayashi, T. (2004). A lipid-specific toxin reveals heterogeneity of sphingomyelin-containing membranes. *Biophysical Journal*, *86*, 296–307. https://doi.org/10.1016/S0006-3495(04)74105-3

Johnson, K. A., Endapally, S., Vazquez, D. C., Infante, R. E., & Radhakrishnan, A. (2019). Ostreolysin A and anthrolysin O use different mechanisms to control movement of cholesterol from the plasma membrane to the endoplasmic reticulum. *Journal of Biological Chemistry*, *294*, 17289–17300. https://doi.org/10.1074/jbc.RA119.010393

Kasahara, K., Kaneda, M., Miki, T., Iida, K., Sekino-Suzuki, N., Kawashima, I., Suzuki, H., Shimonaka, M., Arai, M., Ohno-Iwashita, Y., Kojima, S., Abe, M., Kobayashi, T., Okazaki, T., Souri, M., Ichinose, A., & Yamamoto, N. (2013). Clot retraction is mediated by factor XIII-dependent fibrin-alphaIIbbeta3-myosin axis in platelet sphingomyelin-rich membrane rafts. *Blood*, *122*, 3340–3348. https://doi.org/10.1182/blood-2013-04-491290

Kavishwar, A., Medarova, Z., & Moore, A. (2011). Unique sphingomyelin patches are targets of a beta-cell-specific antibody. *Journal of Lipid Research*, *52*, 1660–1671. https://doi.org/10.1194/jlr.M017582

Kidani, Y., Ohshima, K., Sakai, H., Kohno, T., Baba, A., & Hattori, M. (2012). Differential localization of sphingomyelin synthase isoforms in neurons regulates sphingomyelin cluster formation. *Biochemical and Biophysical Research Communications*, *417*, 1014–1017. https://doi.org/10.1016/j.bbrc.2011.12.079

Kinoshita, M., Goretta, S., Tsuchikawa, H., Matsumori, N., & Murata, M. (2013). Characterization of the ordered phase formed by sphingomyelin analogues and cholesterol binary mixtures. *Biophysics*, *9*, 37–49. https://doi.org/10.2142/biophysics.9.37

Kinoshita, M., Suzuki, K. G., Matsumori, N., Takada, M., Ano, H., Morigaki, K., Abe, M., Makino, A., Kobayashi, T., Hirosawa, K. M., Fujiwara, T. K., Kusumi, A., & Murata, M. (2017). Raft-based sphingomyelin interactions revealed by new fluorescent sphingomyelin analogs. *Journal of Cell Biology*, *216*, 1183–1204. https://doi.org/10.1083/jcb.201607086

Kishimoto, T., Ishitsuka, R., & Kobayashi, T. (2016). Detectors for evaluating the cellular landscape of sphingomyelin- and cholesterol-rich membrane domains. *Biochimica et Biophysica Acta*, *1861*, 812–829. https://doi.org/10.1016/j.bbalip.2016.03.013

Kishimoto, T., Tomishige, N., Murate, M., Ishitsuka, R., Schaller, H., Mely, Y., Ueda, K., & Kobayashi, T. (2020). Cholesterol asymmetry at the tip of filopodia during cell adhesion. *FASEB Journal*, *34*, 6185–6197. https://doi.org/10.1096/fj.201900065RR

Kiyokawa, E., Baba, T., Otsuka, N., Makino, A., Ohno, S., & Kobayashi, T. (2005). Spatial and functional heterogeneity of sphingolipid-rich membrane domains. *Journal of Biological Chemistry*, *280*, 24072–24084. https://doi.org/10.1074/jbc.M502244200

Kiyokawa, E., Makino, A., Ishii, K., Otsuka, N., Yamaji-Hasegawa, A., & Kobayashi, T. (2004). Recognition of sphingomyelin by lysenin and lysenin-related proteins. *Biochemistry*, *43*, 9766–9773. https://doi.org/10.1021/bi049561j

Kristan, K., Podlesek, Z., Hojnik, V., Gutierrez-Aguirre, I., Guncar, G., Turk, D., Gonzalez-Manas, J. M., Lakey, J. H., Macek, P., & Anderluh, G. (2004). Pore formation by equinatoxin, a eukaryotic pore-forming toxin, requires a flexible N-terminal region and a stable beta-sandwich. *Journal of Biological Chemistry*, *279*, 46509–46517. https://doi.org/10.1074/jbc.M406193200

Kulma, M., Herec, M., Grudzinski, W., Anderluh, G., Gruszecki, W. I., Kwiatkowska, K., & Sobota, A. (2010). Sphingomyelin-rich domains are sites of lysenin oligomerization: Implications for raft studies. *Biochimica et Biophysica Acta*, *1798*, 471–481. https://doi.org/10.1016/j.bbamem.2009.12.004

Kulma, M., Kwiatkowska, K., & Sobota, A. (2012). Raft coalescence and FcgammaRIIA activation upon sphingomyelin clustering induced by lysenin. *Cellular Signalling*, *24*, 1641–1647. https://doi.org/10.1016/j.cellsig.2012.04.007

Lazzarini, A., Macchiarulo, A., Floridi, A., Coletti, A., Cataldi, S., Codini, M., Lazzarini, R., Bartoccini, E., Cascianelli, G., Ambesi-Impiombato, F. S., Beccari, T., Curcio, F., & Albi, E. (2015). Very-long-chain fatty acid sphingomyelin in nuclear lipid microdomains of hepatocytes and hepatoma cells: Can the exchange from C24:0 to C16:0 affect signal proteins and vitamin D receptor? *Molecular Biology of the Cell*, *26*, 2418–2425. https://doi.org/10.1091/mbc.e15-04-0229

Leonard, C., Pollet, H., Vermylen, C., Gov, N., Tyteca, D., & Mingeot-Leclercq, M. P. (2018). Tuning of differential lipid order between submicrometric domains and surrounding membrane Upon erythrocyte reshaping. *Cellular Physiology and Biochemistry*, *48*, 2563–2582. https://doi.org/10.1159/000492700

Levental, I., Levental, K. R., & Heberle, F. A. (2020). Lipid rafts: Controversies resolved, mysteries remain. *Trends in Cell Biology*, *30*, 341–353. https://doi.org/10.1016/j.tcb.2020.01.009

Lingwood, D., & Simons, K. (2010). Lipid rafts As a membrane-organizing principle. *Science (New York, N.Y.)*, *327*, 46–50. https://doi.org/10.1126/science.1174621

Makino, A., Abe, M., Ishitsuka, R., Murate, M., Kishimoto, T., Sakai, S., Hullin-Matsuda, F., Shimada, Y., Inaba, T., Miyatake, H., Tanaka, H., Kurahashi, A., Pack, C. G., Kasai, R. S., Kubo, S., Schieber, N. L., Dohmae, N., Tochio, N., & Hagiwara, K.,…, & Kobayashi, T. (2017). A novel sphingomyelin/cholesterol domain-specific probe reveals the dynamics of the membrane domains during virus release and in niemann-pick type C. *FASEB Journal*, *31*, 1301–1322. https://doi.org/10.1096/fj.201500075R

Makino, A., Abe, M., Murate, M., Inaba, T., Yilmaz, N., Hullin-Matsuda, F., Kishimoto, T., Schieber, N. L., Taguchi, T., Arai, H., Anderluh, G., Parton, R. G., & Kobayashi, T. (2015). Visualization of the heterogeneous membrane distribution of sphingomyelin associated with cytokinesis, cell polarity, and sphingolipidosis. *FASEB Journal*, *29*, 477–493. https://doi.org/10.1096/fj.13-247585

Marsh, D. (2013). *Handbook of lipid bilayers*. CRC Press.

Mizuno, H., Abe, M., Dedecker, P., Makino, A., Rocha, S., Ohno-Iwashita, Y., Hofkens, T., Kobayashi, T., & Miyawaki, A. (2011). Fluorescent probes for supersolution imaging of lipid domains on the plasma membrane. *Chemical Science*, *2*, 1548–1553. https://doi.org/10.1039/c1sc00169h

Mound, A., Lozanova, V., Warnon, C., Hermant, M., Robic, J., Guere, C., Vie, K., Lambert de Rouvroit, C., Tyteca, D., Debacq-Chainiaux, F., & Poumay, Y. (2017). Non-senescent keratinocytes organize in plasma membrane submicrometric lipid domains enriched in sphingomyelin and involved in re-epithelialization. *Biochimica et Biophysica Acta*, *1862*, 958–971. https://doi.org/10.1016/j.bbalip.2017.06.001

Murate, M., Abe, M., Kasahara, K., Iwabuchi, K., Umeda, M., & Kobayashi, T. (2015). Transbilayer distribution of lipids at nano scale. *Journal of Cell Science*, *128*, 1627–1638. https://doi.org/10.1242/jcs.163105

Murate, M., Tomishige, N., & Kobayashi, T. (2020). Wrapping axons in mammals and drosophila: Different lipids, same principle. *Biochimie*, *178*, 39–48. https://doi.org/10.1016/j.biochi.2020.08.002

Nakai, Y., Sakurai, Y., Yamaji, A., Asou, H., Umeda, M., Uyemura, K., & Itoh, K. (2000). Lysenin-sphingomyelin binding at the surface of oligodendrocyte lineage cells increases during differentiation in vitro. *Journal of Neuroscience Research*, *62*, 521–529. https://doi.org/10.1002/1097-4547(20001115)62:4<521::AID-JNR6>3.0.CO;2-8

Panevska, A., Hodnik, V., Skocaj, M., Novak, M., Modic, S., Pavlic, I., Podrzaj, S., Zaric, M., Resnik, N., Macek, P., Veranic, P., Razinger, J., & Sepcic, K. (2019a). Pore-forming protein complexes from Pleurotus mushrooms kill western corn rootworm and Colorado potato beetle through targeting membrane ceramide phosphoethanolamine. *Scientific Reports*, *9*, 5073. https://doi.org/10.1038/s41598-019-41450-4

Panevska, A., Skocaj, M., Krizaj, I., Macek, P., & Sepcic, K. (2019b). Ceramide phosphoethanolamine, an enigmatic cellular membrane sphingolipid. *Biochimica et Biophysica Acta*, *1861*, 1284–1292. https://doi.org/10.1016/j.bbamem.2019.05.001

Podobnik, M., Savory, P., Rojko, N., Kisovec, M., Wood, N., Hambley, R., Pugh, J., Wallace, E. J., McNeill, L., Bruce, M., Liko, I., Allison, T. M., Mehmood, S., Yilmaz, N., Kobayashi, T., Gilbert, R. J., Robinson, C. V., Jayasinghe, L., & Anderluh, G., … (2016). Crystal structure of an invertebrate cytolysin pore reveals unique properties and mechanism of

assembly. *Nature Communications*, *7*, 11598. https://doi.org/10.1038/ncomms11598

Rivera-de-Torre, E., Palacios-Ortega, J., Slotte, J. P., Gavilanes, J. G., Martinez-Del-Pozo, A., & Garcia-Linares, S. (2020). Functional and structural variation among sticholysins, pore-forming proteins from the sea anemone stichodactyla helianthus. *International Journal of Molecular Sciences*, *21*, 8915. https://doi.org/10.3390/ijms21238915

Rojko, N., Cronin, B., Danial, J. S., Baker, M. A., Anderluh, G., & Wallace, M. I. (2014). Imaging the lipid-phase-dependent pore formation of equinatoxin II in droplet interface bilayers. *Biophysical Journal*, *106*, 1630–1637. https://doi.org/10.1016/j.bpj.2013.11.4507

Rojko, N., Dalla Serra, M., Macek, P., & Anderluh, G. (2016). Pore formation by actinoporins, cytolysins from sea anemones. *Biochimica et Biophysica Acta*, *1858*, 446–456. https://doi.org/10.1016/j.bbamem.2015.09.007

Rojko, N., Kristan, K. C., Viero, G., Zerovnik, E., Macek, P., Dalla Serra, M., & Anderluh, G. (2013). Membrane damage by an alpha-helical pore-forming protein, equinatoxin II, proceeds through a succession of ordered steps. *Journal of Biological Chemistry*, *288*, 23704–23715. https://doi.org/10.1074/jbc.M113.481572

Shogomori, H., & Kobayashi, T. (2008). Lysenin: A sphingomyelin specific pore-forming toxin. *Biochimica et Biophysica Acta*, *1780*, 612–618. https://doi.org/10.1016/j.bbagen.2007.09.001

Skocaj, M., Resnik, N., Grundner, M., Ota, K., Rojko, N., Hodnik, V., Anderluh, G., Sobota, A., Macek, P., Veranic, P., & Sepcic, K. (2014). Tracking cholesterol/sphingomyelin-rich membrane domains with the ostreolysin A-mCherry protein. *PloS one*, *9*, e92783. https://doi.org/10.1371/journal.pone.0092783

Skocaj, M., Yu, Y., Grundner, M., Resnik, N., Bedina Zavec, A., Leonardi, A., Krizaj, I., Guella, G., Macek, P., Kreft, M. E., Frangez, R., Veranic, P., & Sepcic, K. (2016). Characterisation of plasmalemmal shedding of vesicles induced by the cholesterol/sphingomyelin binding protein, ostreolysin A-mCherry. *Biochimica et Biophysica Acta*, *1858*, 2882–2893. https://doi.org/10.1016/j.bbamem.2016.08.015

Taksir, T. V., Johnson, J., Maloney, C. L., Yandl, E., Griffiths, D., Thurberg, B. L., & Ryan, S. (2012). Optimization of a histopathological biomarker for sphingomyelin accumulation in acid sphingomyelinase deficiency. *Journal of Histochemistry and Cytochemistry*, *60*, 620–629. https://doi.org/10.1369/0022155412451129

Tomishige, N., Murate, M., Didier, P., Richert, L., Mely, Y., & Kobayashi, T. (2021). The use of pore-forming toxins to image lipids and lipid domains. *Methods in Enzymology*, *649*, 503–542. https://doi.org/10.1016/bs.mie.2021.01.019

Wang, T., Shogomori, H., Hara, M., Yamada, T., & Kobayashi, T. (2012). Nanomechanical recognition of sphingomyelin-rich membrane domains by atomic force microscopy. *Biochemistry*, *51*, 74–82. https://doi.org/10.1021/bi2011652

Yachi, R., Uchida, Y., Balakrishna, B. H., Anderluh, G., Kobayashi, T., Taguchi, T., & Arai, H. (2012). Subcellular localization of sphingomyelin revealed by two toxin-based probes in mammalian cells. *Genes to Cells*, *17*, 720–727. https://doi.org/10.1111/j.1365-2443.2012.01621.x

Yamaji, A., Sekizawa, Y., Emoto, K., Sakuraba, H., Inoue, K., Kobayashi, H., & Umeda, M. (1998). Lysenin, a novel sphingomyelin-specific binding protein. *Journal of Biological Chemistry*, *273*, 5300–5306. https://doi.org/10.1074/jbc.273.9.5300

Yamaji-Hasegawa, A., Hullin-Matsuda, F., Greimel, P., & Kobayashi, T. (2016). Pore-forming toxins: Properties, diversity, and uses as tools to image sphingomyelin and ceramide phosphoethanolamine. *Biochimica et Biophysica Acta*, *1858*, 576–592. https://doi.org/10.1016/j.bbamem.2015.10.012

Yamaji-Hasegawa, A., Makino, A., Baba, T., Senoh, Y., Kimura-Suda, H., Sato, S. B., Terada, N., Ohno, S., Kiyokawa, E., Umeda, M., & Kobayashi, T. (2003). Oligomerization and pore formation of a sphingomyelin-specific toxin, lysenin. *Journal of Biological Chemistry*, *278*, 22762–22770. https://doi.org/10.1074/jbc.M213209200

Yilmaz, N., & Kobayashi, T. (2015). Visualization of lipid membrane reorganization induced by a pore-forming toxin using high-speed atomic force microscopy. *ACS Nano*, *9*, 7960–7967. https://doi.org/10.1021/acsnano.5b01041

Yilmaz, N., Yamada, T., Greimel, P., Uchihashi, T., Ando, T., & Kobayashi, T. (2013). Real time visualization of assembling of a sphingomyelin-specific toxin on planar lipid membranes. *Biophysical Journal*, *105*, 1397–1405. https://doi.org/10.1016/j.bpj.2013.07.052

Yilmaz, N., Yamaji-Hasegawa, A., Hullin-Matsuda, F., & Kobayashi, T. (2018). Molecular mechanisms of action of sphingomyelin-specific pore-forming toxin, lysenin. *Seminars in Cell and Developmental Biology*, *73*, 188–198. https://doi.org/10.1016/j.semcdb.2017.07.036

Yoshida, Y., Yoneda, K., Umeda, M., Ide, C., & Fujimoto, K. (2001). Localization of sphingomyelin during the development of dorsal and tail epidermis of mice. *British Journal of Dermatology*, *145*, 758–770. https://doi.org/10.1046/j.1365-2133.2001.04489.x